

## SPECTRAL AND INTERMITTENCY PROPERTIES OF RELATIVISTIC TURBULENCE

JONATHAN ZRAKE AND ANDREW I. MACFADYEN

Center for Cosmology and Particle Physics, Physics Department, New York University, New York, NY 10003, USA  
*Draft version November 1, 2018*

### ABSTRACT

High-resolution numerical simulations are utilized to examine isotropic turbulence in a compressible fluid when long wavelength velocity fluctuations approach light speed. Spectral analysis reveals an inertial sub-range of relativistic motions with a broadly 5/3 index. The use of generalized Lorentz-covariant structure functions based on the four-velocity is proposed. These structure functions extend the She-Leveque model for intermittency into the relativistic regime.

*Subject headings:* hydrodynamics — methods: numerical — gamma-ray burst: general — turbulence

### 1. INTRODUCTION

A rapidly accumulating body of astronomical observations indicates the presence of relativistic turbulence in a variety of astrophysical systems. Cosmological gamma-ray bursts (GRBs) accelerate relativistic jets with energies exceeding the kinetic energy of a supernova ( $10^{51-52}$  ergs) to Lorentz factors  $\gamma \gtrsim 100$  and contain internal fluctuations with  $\delta\gamma \sim 2$  (Piran 2004), while jets from active galactic nuclei and micro-quasars are found to have  $\gamma \gtrsim 10$  and  $\gamma \lesssim 2$  respectively. Recent discoveries indicate that a broad class of stellar explosions, including those associated with X-ray transients and low-luminosity GRBs (Kulkarni et al. 1998; Starling et al. 2011), and even some supernovae lacking high-energy emission (Soderberg et al. 2010; Paragi et al. 2010), also accelerate significant amounts of relativistic material. These relativistic flows are highly susceptible to turbulence due to the extremely high inferred Reynolds numbers and the abundant presence of shear due to observed flow asymmetries.

In recent models for fluctuating emission from GRBs, the relativistic turbulence is proposed to be directly observable, as relativistic eddies beam their radiation into narrow cones which sweep by the observers' line of sight (Narayan & Kumar 2009; Lazar et al. 2009). In addition, the central engine for short-duration GRBs likely involves the turbulent merging of neutron stars which are known sources of gravitational radiation (Hulse & Taylor 1975). Knowledge of the properties of turbulence present in these sources (Melatos & Peralta 2010) may aid with detection and interpretation of gravitational waves from these sources when interferometers such as advanced LIGO become operable in the near future. Relativistic turbulence is also likely generated by phase transitions in the early universe and may be produced in heavy ion colliders and laser experiments.

The fundamental properties of kinematically relativistic hydrodynamic turbulence have not, until now, been investigated. Turbulence in fully relativistic MHD has been studied for decaying (Zhang et al. 2009; Inoue et al. 2011; Beckwith & Stone 2011) and driven (Zrake & MacFadyen 2011, 2012) flows. Also, simulations ignoring the uid rest mass have been done in the magnetized (Cho 2005) and unmagnetized (Radice & Rezzolla 2012) cases. Fundamental questions

relating to the non-linear behavior of the SRHD system remain to be answered. For example, it has not previously been known whether relativistic velocity excitations survive to small scales or are suppressed near the outer scales of a turbulent flow. If relativistic motions persist deeply into the cascade, then universal behavior may be expected. However, relativistic statistical measures are required to characterize its scaling and intermittency properties. For example, the power spectrum of three-velocity cannot obey a power law above the scale  $\ell_\gamma$  where the velocity differences asymptotically approach light speed. Traditional two-point structure functions also break down at scales  $\ell > \ell_\gamma$ . Statistical diagnostics built on the fluid four-velocity,  $u = (\gamma c, \gamma \mathbf{v})$ , are thus needed.

In this Letter, we present high-resolution simulations of isotropic relativistic turbulence and introduce Lorentz covariant scaling diagnostics to analyze its basic properties. Questions to be addressed include (1) Does relativistic turbulence display universal behavior? (2) Can its intermittency be described in terms of known phenomenological models? (3) How deeply into the cascade do velocity fluctuations remain relativistic?

In order to address these questions, numerical integrations of the special relativistic hydrodynamics (SRHD) equations were conducted on the Pleiades supercomputer at the Ames research center on lattice sizes up to  $2048^3$ , utilizing more than 2,000,000 CPU-hours. The SRHD equations are cast in conservation form for the particle number  $\nabla_\nu N^\nu = 0$  and energy-momentum tensor  $\nabla_\nu T^{\mu\nu} = S^\mu$  and closed by the adiabatic equation of state  $p = \rho e(\Gamma - 1)$  where  $\Gamma = 4/3$ ,  $e$  is the specific internal energy,  $\rho$  is the co-moving mass density and  $T^{\mu\nu} = \rho h u^\mu u^\nu + p g^{\mu\nu}$ , and  $h = c^2 + e + p/\rho$ . The source term  $S^\mu = \rho a^\mu - \rho(e/e_0)^4 u^\mu$  includes injection of energy and momentum at the large scales and the subtraction of internal energy (with parameter  $e_0 = 0.25$ ) to permit stationary evolution. Vortical modes at  $k/2\pi \leq 3$  are forced by the four-acceleration field  $a^\mu = \frac{du^\mu}{d\tau}$  which smoothly decorrelates over a large-eddy turnover time, as described in Zrake & MacFadyen (2012). The numerical scheme employed is the 5th-order accurate weighted essentially non-oscillatory (WENO) conservative finite-difference scheme which has been extensively tested for SRHD (Zhang & MacFadyen 2006) and is implemented

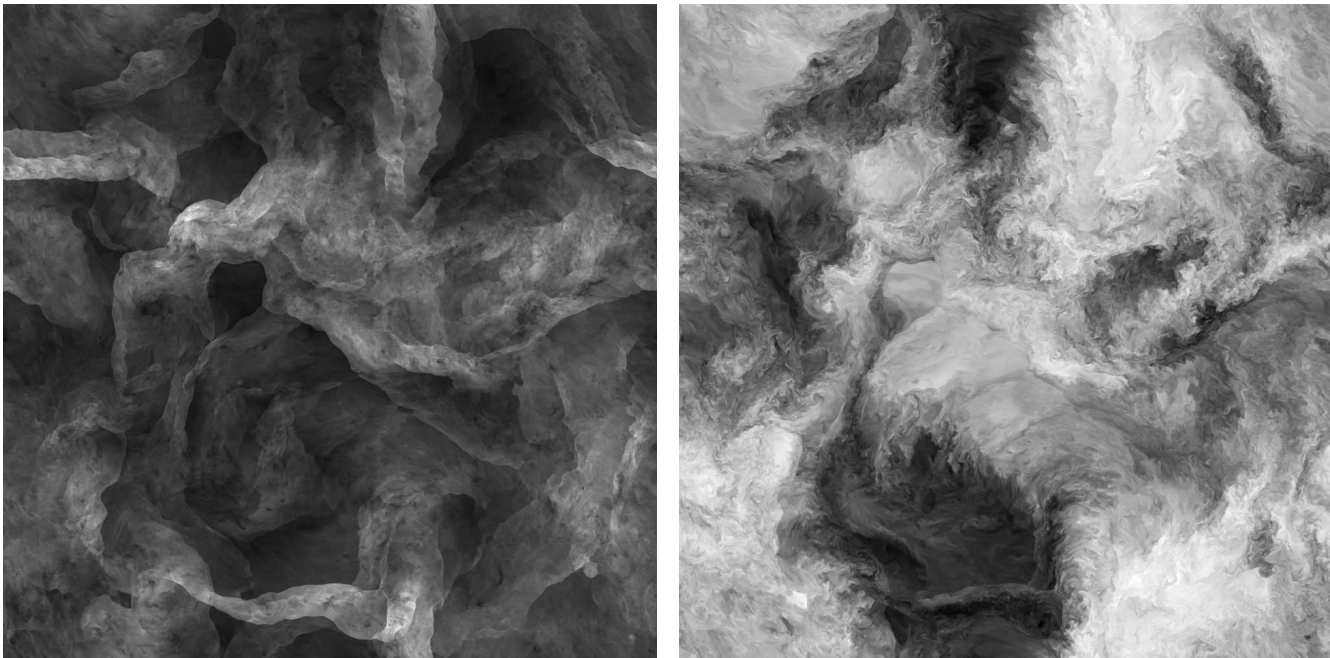


**Figure 1.** Slices of the co-moving density (left) and four-velocity component out of the page (right), indicating the structure of isotropic relativistic turbulence at a resolution of  $2048^3$ . Density is scaled to the  $1/2$  power to elucidate structures in the evacuated regions. The grayscale is from minimum (darkest) to maximum (brightest).

in the Mara code (Zrake & MacFadyen 2012) with improved smoothness indicators (Shen & Zha 2010). The simulations take place on the periodic cube of size  $L$ , and were evolved at stationarity for at least 5 large eddy turnover times, with the exception of the  $2048^3$  run which was evolved for  $1/2$  of a turnover time. Each model at resolution  $N^3$  was initialized from stationary turbulence at resolution  $(N/2)^3$ , after which a full turnover time is required to re-establish stationarity. Table 1 summarizes the simulation parameters for the  $2048^3$  run.

## 2. RESULTS

Images of the fully developed turbulent fields are shown in Fig. 1. The co-moving density (left panel) contains fluctuations above and below the mean by factors of 16. The highest density structures are sheet-like, but not fully two-dimensional and trace the front between clouds of fluid colliding with relativistic velocities. Shocks and contact discontinuities are evident where the density field changes abruptly. In compressible turbulence, these shocks indicate the geometry of the most aggressively dissipating structures (Kritsuk et al. 2007). These shocks are more intense in a relativistic gas because their density contrasts may be arbitrarily large,  $\sigma = \frac{\Gamma+1}{\Gamma-1} + \frac{\Gamma}{\Gamma-1}e/c^2$  whereas in the non-relativistic limit the density ratio is bounded by  $\frac{\Gamma+1}{\Gamma-1}$ . The transverse four-velocity component (right panel) reveals a highly structured hierarchy of shearing motions down to the smallest scales. It also exhibits remarkable coherence over some regions, where large clouds of fluid are in relativistic motion into (or out of) the page. Fluid elements separated by  $1/100$ ,  $1/10$  and  $1/5$  of the image are, on average, in relative motion with four-velocities of  $1/2$ ,  $1$  and  $2$  respectively.

Turbulent flows at sufficiently large Reynolds number are known to contain a range of scales over which the

**Table 1**  
Simulation parameters

Parameter	Symbol	Value
Box size	$L$	-
Driving scale scale	-	$L/2$
Relativistic scale	$\ell_\gamma$	$0.16L$
Mean pairwise-relative Lorentz factor	$\bar{\gamma}_{rel}$	3.10
Mean lab-frame Lorentz factor	$\bar{\gamma}$	1.67
Max lab-frame Lorentz factor	$\gamma_{max}$	5.73
Mean relativistic Mach number	$\mathcal{M}$	2.67
Max relativistic Mach number	$\mathcal{M}_{max}$	22.9
Mean pressure to mean density ratio	$\bar{p}/\bar{\rho}c^2$	0.41
Lower 1% density quantile	-	$0.027\bar{p}$
Upper 1% density quantile	-	$4.89\bar{p}$

**Note.** — Simulation parameters are taken from the  $2048^3$  run. The relativistic Mach number is defined to be  $\mathcal{M} = (\gamma\beta)_{fluid}/(\gamma\beta)_{sound}$ . Quantities with over-bars are volume averaged at each iteration, and all quantities are time-averaged during stationary evolution.

behavior is universal, i.e. statistically independent of energy injection and dissipation effects at the largest and smallest scales respectively. This range is referred to as the inertial sub-interval, and is often identified by self-similar behavior in the power spectrum  $P(k)$  of the velocity field. The 1941 theory of Kolmogorov (K41) (Kolmogorov 1941) for incompressible, non-relativistic turbulence predicts that  $P(k) \propto k^{-5/3}$  in the inertial interval. In relativistic flows the amplitude of velocity fluctuations cannot exceed  $c$ , so the power spectrum of velocity cannot obey a power law to arbitrarily large scales. However, the physics of a relativistic cascade may still be universal, and it could be revealed by an appropriate choice of generalized diagnostics, such as the power spectrum of fluid four-velocity.

Figs. 2a and 2b show the power spectrum  $P(k)$  of four-

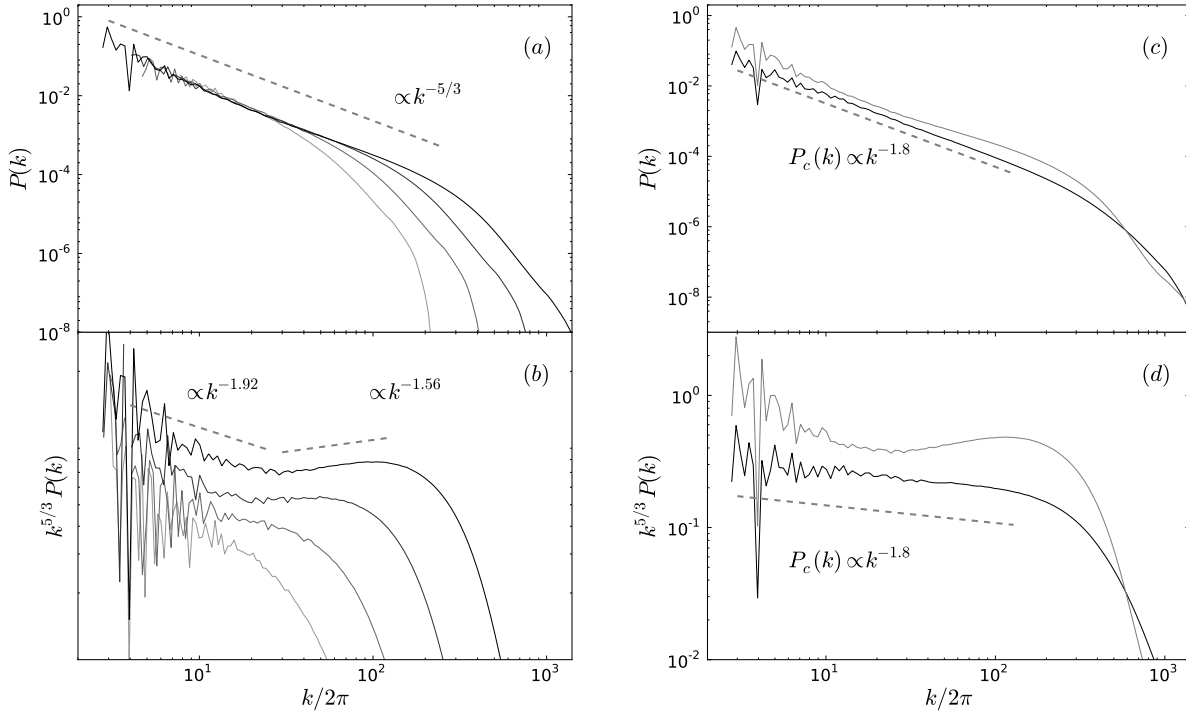


**Figure 2.** (a) Power spectrum of the four-velocity field at resolutions  $256^3$ ,  $512^3$ ,  $1024^3$ , and  $2048^3$  (increasing in weight from gray to black). (b) The same data as in (a) but compensated by  $k^{5/3}$  and offset, stretched to exaggerate deviations from a 5/3 law. An arbitrary vertical offset is given to each curve in order to clarify the spectral shape between  $k/2\pi (= 1/L) = 10$  and 100. (c) Power spectrum of the Helmholtz decomposed four-velocity field. The compressive component  $P_c(k)$  (black) follows a power law with index 1.80. (d) The same data as in (c) but compensated by  $k^{5/3}$ .

velocity at lattice sizes of  $256^3$ ,  $512^3$ ,  $1024^3$ , and  $2048^3$ , where

$$P(k)dk = \sum_{\mathbf{k} \in dk} \tilde{\mathbf{u}}_{\mathbf{k}} \cdot \tilde{\mathbf{u}}_{\mathbf{k}}^* \quad (1)$$

is computed from the discrete Fourier transform

$$\tilde{\mathbf{u}}_{\mathbf{k}}^{\mu} = \frac{1}{N^3} \sum_{l,m,n} u^{\mu}(\mathbf{x}_{l,m,n}) e^{-i\mathbf{k} \cdot \mathbf{x}_{l,m,n}} \quad (2)$$

of the four-velocity field. Throughout the text, boldface is used to denote the spatial components of a four-vector. The normalization by  $N^3$ , where  $N$  is the number of lattice points per direction, guarantees that  $P(k)$  satisfies  $\int P(k)dk = \langle \mathbf{u} \cdot \mathbf{u} \rangle$ . We find evidence for an inertial interval of relativistic velocity fluctuations between 1/10 and 1/100 of the largest scale. As the resolution increases from  $256^3$  to  $1024^3$ , a short interval obeying the 5/3 law emerges. But the subsequent resolution of  $2048^3$  reveals a more featureful spectrum of four-velocity, consisting of a broken power-law which is steeper (1.92) at the largest scales and shallower (1.56) at moderate scales. This may be due to the bottleneck effect which is characterized by an accumulation of power at the small-scale end of the inertial range (Falkovich 1994). There has been substantial effort to distinguish true inertial scaling from the contamination of bottlenecks (Beresnyak & Lazarian 2009). We report that the power spectrum of four-velocity is *broadly* 5/3, owing to the fact that each higher resolution adds additional scales which, on the average, obey 5/3 scaling. In relativistic turbulence, asymptotically converged scaling behavior may not yield a single power law. This

is because a relativistic cascade contains a new dimensionless number, the Lorentz factor, at each scale. As a simple illustration, a cursory application of the K41 dimensional argument to relativistic eddies reveals that the Lorentz factor at a scale  $\ell$  satisfies

$$\frac{(\gamma_{\ell} - 1)^3(\gamma_{\ell} + 1)}{\gamma_{\ell}^2} = C\epsilon^2 \ell^2 / c^6. \quad (3)$$

where  $\epsilon$  is the energy injection rate per unit mass and  $C$  is analogous to the Kolmogorov constant. This relation does not admit a single power law solution. Instead, solutions are  $\gamma_{\ell} \propto \ell$  for large  $\gamma$ , and  $\gamma_{\ell} \propto \ell^{2/3}$  for small  $\gamma$ .

Unlike the total fluid four-velocity, the compressive four-velocity component  $u_c^{\mu}$  is strictly self-similar over the inertial interval. This is evidence that a local cascade of acoustic modes is operating across those scales. The Helmholtz decomposition of spatial components of four-velocity is done in the Fourier domain, with the compressive part  $\tilde{\mathbf{u}}_{\mathbf{k}}^c = \tilde{\mathbf{u}}_{\mathbf{k}} \cdot \mathbf{k}/k$  and the solenoidal part  $\tilde{\mathbf{u}}_{\mathbf{k}}^s = \tilde{\mathbf{u}}_{\mathbf{k}} - \tilde{\mathbf{u}}_{\mathbf{k}}^c$ . As shown in Figs. 2c and 2d, the power-law range of dilatational power spectrum  $P_c(k)$  extends through the energy injection scale. This is because only the vortical modes are being directly excited. Its slope is 1.80, which is in contrast with the supersonic limit of highly compressible turbulence, where all the compressive power is in shocks, and the dilatational power spectrum  $P_c(k) \propto k^{-2}$ . The power spectrum of solenoidal  $P_s(k)$  four-velocity is not at all self-similar, and accounts for the majority of power (82%) throughout the cascade. We remark that thermally relativistic

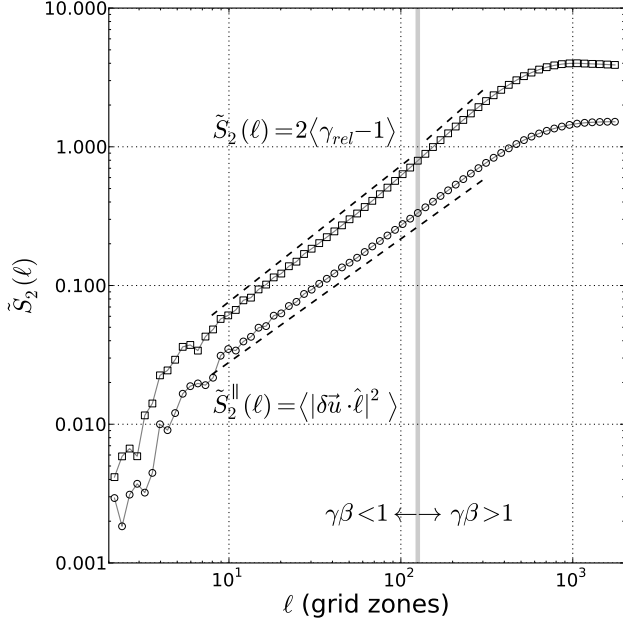


**Figure 3.** The generalized structure functions of four-velocity  $\tilde{S}_2^{\parallel}(\ell)$  (longitudinal projection, squares) and  $\tilde{S}_2(\ell)$  (circles) as a function of the separation  $\ell$  for resolution 2048<sup>3</sup>. The vertical gray bar marks the relativistic scale  $\ell_\gamma = 0.06L$ , below which velocity fluctuations become sub-relativistic.

tic turbulence admits a novel mechanism for energy exchange between the vortical and compressive motions of the fluid. The mechanical work done in compressing a fluid volume goes into internal energy, which for a relativistic gas enhances its inertia through the coupling of total enthalpy to fluid four-velocity expressed by the term  $\rho h u^\mu u^\nu$  in the energy-momentum tensor. This additional mechanism of energy transfer adds qualitatively new dynamics to the turbulent cascade. In particular, it may break the statistical decoupling between the compressive and vortical cascades that was recently discovered for non-relativistic compressible turbulence (Aluie 2011). The signature of this effect is proposed to be an enhanced coherency among the phases of similar-scale shearing and dilating velocity modes, that can be determined from the bi-spectrum of fluid four-velocity.

Modern descriptions of turbulence have recognized that two-point correlations of velocity are not normally distributed around the mean fluctuating fluid velocity (Kolmogorov 1962; Kraichnan 1990; Cao et al. 1996). This effect is referred to as intermittency, and represents an important departure from the K41 theory. Intermittency may be quantified by examining higher moments of the probability distribution function (PDF) of the velocity increments at various scales  $\ell$ . In particular, the 1994 model of She-Leveque (SL94) (She & Leveque 1994) has had great success in predicting the scaling exponents  $\zeta_p$  for the velocity structure functions  $S_p(\ell)$  of order  $p$ . We have found that relativistic turbulence also displays intermittency, and that the SL94 model provides an excellent description, provided that velocity increments are properly defined to accommodate relativistic fluctuations. We generalize the total velocity structure function as

$$\tilde{S}_p(\ell) = \langle |\delta u^\mu \delta u_\mu|^{p/2} \rangle \quad (4)$$

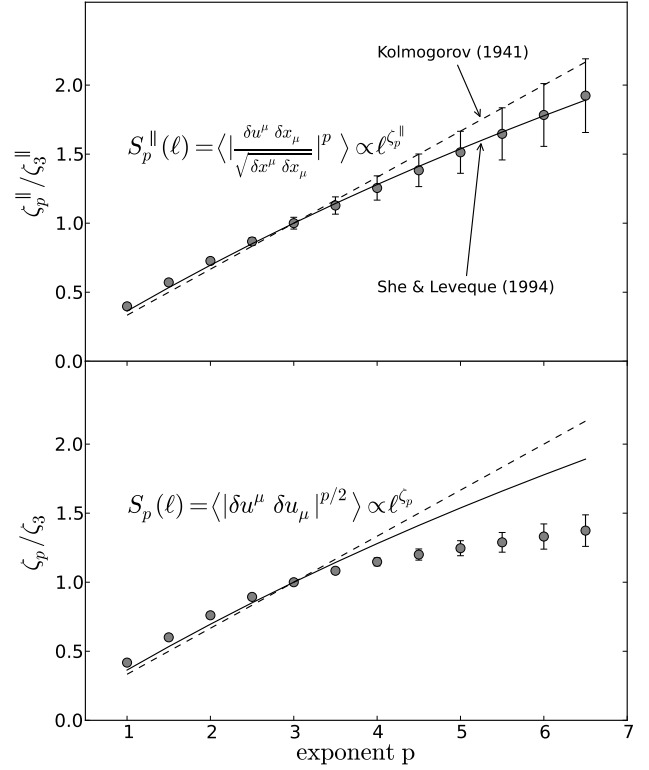


**Figure 4.** Dependence of  $\zeta_p$  on the exponent  $p$  for the power-law scaling of longitudinal  $\tilde{S}_p^{\parallel}(\ell)$  (top) and total  $\tilde{S}_p(\ell)$  (bottom) structure functions.  $\zeta_p$  is obtained by a least-squares fit of the structure functions between  $\ell = 1/10$  and  $1/100$  of the domain. All the scaling exponents are normalized by  $\zeta_3$ . Error bars indicate the standard deviation over 6 equally-spaced stationary snapshots at 1024<sup>3</sup>. The intermittency models of K41 and SL94 are shown in dashed and solid lines respectively.

where  $\delta u^\mu = u_2^\mu - u_1^\mu$  and  $\ell = (\delta x^\mu \delta x_\mu)^{1/2}$ . Four-velocity pairs are chosen to be simultaneous in the global center-of-momentum frame so that  $\delta x^0 = 0$ . Note that  $\tilde{S}_p(\ell) = \langle |2(\gamma_{rel} - 1)|^{p/2} \rangle$  where  $\gamma_{rel}$  is the Lorentz factor of one fluid element as measured in the rest frame of the other.  $\tilde{S}_p(\ell)$  becomes  $\langle |\mathbf{v}_2 - \mathbf{v}_1|^p \rangle$  in the non-relativistic limit. We also generalize the longitudinal structure function

$$\tilde{S}_p^{\parallel}(\ell) = \langle \left| \frac{\delta u^\mu \delta x_\mu}{(\delta x^\mu \delta x_\mu)^{1/2}} \right|^p \rangle \quad (5)$$

which can also be written as  $\langle |\delta \mathbf{u} \cdot \hat{\ell}|^p \rangle$ , where  $\hat{\ell} = \boldsymbol{\ell}/\ell$ , because of pair simultaneity.

We utilize  $\tilde{S}_2(\ell)$  to determine the scale  $\ell_\gamma$  to which relativistic velocity fluctuations persist. The kinematic effects of relativity are important when the *relative* four-velocity  $\gamma\beta$  between fluid elements exceeds 1, i.e.  $\langle \gamma_{rel} \rangle > \sqrt{2}$  (or  $\tilde{S}_2(\ell) = 2\sqrt{2} - 2 \approx 0.83$ ). As shown in Fig. 3, this occurs at  $\ell_\gamma = 0.06$ , or 1/16 of the outermost scale.  $\tilde{S}_2(\ell)$  shows two regimes of power-law scaling, having exponents of  $\zeta_2 = 0.98$  below  $\ell_\gamma$  and  $\zeta_2 = 1.09$  above  $\ell_\gamma$ . The longitudinal structure function  $\tilde{S}_2^{\parallel}(\ell)$  obeys a power law with index  $\zeta_2^{\parallel} = 0.89$  between 1/10 and 1/100 of the domain. This is steep relative to the K41 theory for incompressible non-relativistic turbulence that predicts  $\zeta_2 = 2/3$ , but is in close agreement with what was found

in simulations of highly compressible non-relativistic turbulence (Kritsuk et al. 2007).

We find that the SL94 intermittency model extends to relativistic turbulence when the structure function is given by Eqn. 4. Fig. 4 shows that the normalized exponents  $\zeta_p^{\parallel}/\zeta_3^{\parallel}$  through  $p = 6.5$  are well described by the SL94 relation  $\zeta_p = p/9 + 2 - 2(2/3)^{p/3}$ . Error bars are obtained from the standard deviation over 6 snapshots at  $1024^3$ . The total structure function given in Eqn. 5, which measures the statistics of pairwise relative Lorentz factor, exhibits a far greater degree of intermittency. We propose that a new intermittency model for the statistics of relative four-velocities is required, noting that these statistics are inherently non-Gaussian from consideration of relativistic kinematics alone. That is to say, a Gaussian random velocity field does not yield a Gaussian PDF of  $\gamma_{rel}$ , owing to the non-additive nature of Lorentz boosts. A subsequent investigation will examine the shape of the  $\tilde{S}_p(\ell)$  PDF at fixed scales in order to more specifically characterize the source of the intermittency seen in Fig. 4.

### 3. DISCUSSION

In this Letter we have described a numerical investigation of isotropic turbulence in a kinematically and thermally relativistic fluid. It is found that relativistic fluctuations persist to  $1/16$  of the outermost scale. Spectral analysis reveals an inertial sub-range of relativistic velocity fluctuations with a broadly  $5/3$  index. The compressive component of the four-velocity field obeys power-law scaling with index 1.80 over nearly two decades. The SL94 phenomenology successfully describes intermittency in relativistic turbulence, provided the correct definition for the velocity increments is used.

In closing, we remark that for sufficiently large Reynolds number,  $\ell_\gamma$  is larger than the dissipation scale  $\eta$  so that kinetic energy must be transmitted through a sub-relativistic cascade before being thermalized. In this case the ratio  $\ell_\gamma/L$  may be independent of the dissipation mechanism, and should thus be dictated solely by the Lorentz factor of the energy bearing eddies. The exact functional form of this dependence could be constrained by a parameter study over the outer scale Lorentz factor. Doing so would yield insight into the nature of astrophys-

ical turbulent cascades operating far into the relativistic regime.

This research was supported in part by the NSF through grant AST-1009863 and by NASA through grant NNX10AF62G issued through the Astrophysics Theory Program. Resources supporting this work were provided by the NASA High-End Computing (HEC) Program through the NASA Advanced Supercomputing (NAS) Division at Ames Research Center. We thank Andrei Gruzinov and Paul Duffell for insightful discussions.

### REFERENCES

- Aluie, H. 2011, *Phys. Rev. Lett.*, 106, 174502  
 Beckwith, K., & Stone, J. M. 2011, *ApJS*, 193, 6  
 Beresnyak, A., & Lazarian, A. 2009, *ApJ*, 702, 1190  
 Cao, N., Chen, S., & Sreenivasan, K. R. 1996, *Phys. Rev. Lett.*, 77, 3799  
 Cho, J. 2005, *ApJ*, 621, 324  
 Falkovich, G. 1994, *Phys Fluids*, 6, 1411  
 Hulse, R. A., & Taylor, J. H. 1975, *ApJ*, 195, L51  
 Inoue, T., Asano, K., & Ioka, K. 2011, *ApJ*, 734, 77  
 Kolmogorov, A. N. 1941, *Proceedings: Mathematical and Physical Sciences*, 434, 9  
 —. 1962, *J Fluid Mech*, 13, 82  
 Kraichnan, R. H. 1990, *Physical Review Letters (ISSN 0031-9007)*, 65, 575  
 Kritsuk, A. G., Norman, M. L., Padoan, P., & Wagner, R. 2007, *The Astrophysical Journal*, 665, 416  
 Kulkarni, S. R., Frail, D. A., Wieringa, M. H., et al. 1998, *Nature*, 395, 663  
 Lazar, A., Nakar, E., & Piran, T. 2009, *ApJ*, 695, L10  
 Melatos, A., & Peralta, C. 2010, *ApJ*, 709, 77  
 Narayan, R., & Kumar, P. 2009, *MNRAS*, 394, L117  
 Paragi, Z., Taylor, G. B., Kouveliotou, C., et al. 2010, *Nature*, 463, 516  
 Piran, T. 2004, *Rev Mod Phys*, 76, 1143  
 Radice, D., & Rezzolla, L. 2012, *arXiv, astro-ph.HE*  
 She, Z.-S., & Leveque, E. 1994, *Phys. Rev. Lett.*, 72, 336  
 Shen, Y., & Zha, G. 2010, *Int J Numer Meth Fl*, 64, 653  
 Soderberg, A. M., Chakraborti, S., Pignata, G., et al. 2010, *Nature*, 463, 513  
 Starling, R. L. C., Wiersema, K., Levan, A. J., et al. 2011, *MNRAS*, 411, 2792  
 Zhang, W., MacFadyen, A., & Wang, P. 2009, *ApJ*, 692, L40  
 Zhang, W., & MacFadyen, A. I. 2006, *ApJSSeries*, 164, 255  
 Zrake, J., & MacFadyen, A. 2011, *Gamma Ray Bursts 2010. AIP Conference Proceedings*, 1358, 102  
 Zrake, J., & MacFadyen, A. I. 2012, *ApJ*, 744, 32